DETERMINING WETTABILITY FROM *IN SITU* PRESSURE AND SATURATION MEASUREMENTS

Brautaset, A.*, Ersland, G., Graue, A.
Department of Physics and Technology, University of Bergen, Norway
** Now at Statoil*

This paper was prepared for presentation at the International Symposium of the Society of Core Analysts held in Halifax, Nova Scotia, Canada, 4-7 October, 2010

ABSTRACT

During waterfloods of four Portland Chalk core samples at different wettabilities, high spatial resolution Magnetic Resonance Imaging (MRI) was used to measure local *in situ* fluid saturations. Simultaneously, local *in situ* pressures were measured using pressure ports embedded into the core samples at selected positions. The *in situ* pressure response during low pressure waterfloods identified the zero point in the dynamic capillary pressure curve. Local wettability characterization by *in situ* Amott Indices was calculated from these experimental data. The *in situ* Amott Indices corroborated the conventional Amott Index measurements. The waterflood of one of the core samples was simulated using a core flood simulator.

INTRODUCTION

Wettability controls the multiphase fluid flow behavior in an oil reservoir. Information on the wettability of the reservoir rock will improve predictions of total oil recovery, determine fluid flow mechanisms, assist in deciding production strategies and help predicting EOR potential (Donaldson and Thomas, 1969, Morrow, 1990). Improvements in measuring *in situ* wettability are desirable to ensure that various aging techniques provide a homogeneous wettability distribution to avoid artifacts in subsequent EOR studies. The objective of this study was to measure the wettability directly from the *in situ* data by identifying the saturation where the dynamic capillary pressure was zero. The *in situ* wettability measure provided an added benefit in our attempts to calculate relative permeability and dynamic capillary pressure from *in situ* pressure and saturation data (Brautaset *et al*., 2008).

EXPERIMENTAL

Four 8 cm long Portland chalk (Ekdale and Bromley, 1993) core samples were dried for two days at 90°C, vacuum evacuated and saturated with synthetic brine. Porosity was calculated by mass balance. Absolute permeability was measured at different injection rates using a triaxial core holder. Three of the core samples were drained to S_{wi} and aged using low rate injection of crude oil at 80°C to obtain less water-wet conditions. The ageing method provides stable, uniform and reproducible wettability conditions (Graue, 1994, Graue *et al.*, 1998, Graue *et al.*, 1999, Graue *et al.*, 2002, Aspenes *et al.*, 2003). One core sample was left at strongly water-wet conditions. Basic core properties and Amott Indices after ageing are summarized in Table 1. The Amott Index (Amott, 1959) is

a measure of the average wettability conditions of a core sample, ranging from -1 for strongly oil-wet conditions to +1 for strongly water-wet conditions. The Amott Index to water, $I_{w,}$ is the fraction of volume of oil produced from spontaneous imbibition to the total volume of oil produced by spontaneous and forced imbibition combined. The four core samples were prepared for the MRI experiments by substituting brine with deuterium oxide (D_2O) brine in order to determine oil saturation from the measured MRI intensities.

Table 1. Core Properties.

Core Name	Porosity [%]	Permeability [mD]	Amott Index [frac.]
E4	45.6	2.98	0.17
M3	48.2	3.27	0.39
M8	47.3	3.56	0.45
T3	49.0	3.13	1.00

The cores were drained with n-Decane at 2 bar/cm to reach S_{wi} and epoxy coated with end pieces made of Polyoxymethylene (POM); mounted on each end of the cores. Two 3/16" diameter holes were drilled through the epoxy and a 1/8" diameter, five mm deep hole was drilled at the bottom of each 3/16" hole. Plastic tubes were inserted into the 1/8" holes, and the 3/16" holes were filled with silicone to seal the space between the tubes and the core. The pressure ports were localized at 1.5 cm from each core face (see Figure 1). A top layer of epoxy was added to prevent leakage. The plastic tubes were connected to pressure transducers. Fluid properties at relevant temperatures and pressures are listed in Table 2. During constant pressure waterfloods, *in situ* fluid saturation distributions and local pressures were measured simultaneously to obtain local fluid dynamics in the vicinity of the pressure ports. A schematic of the experimental setup is shown in Figure 1.

Table 2. Fluid Properties.

Fluid	Composition	Density, 20°C[g/cm^3]	Viscosity 20°C [cP]	Viscosity 80°C [cP]
Brine	5.0 wt% NaCl and 3.8 wt% $CaCl_2$ 0.1 wt% NaN_3	1.05	1.09	-
D_2O Brine	5 wt% NaCl and 3.8 wt% $CaCl_2$	1.18	1.10	-
Crude oil	-	0.85	14.3	2.7
n-Decane	-	0.73	0.92	-

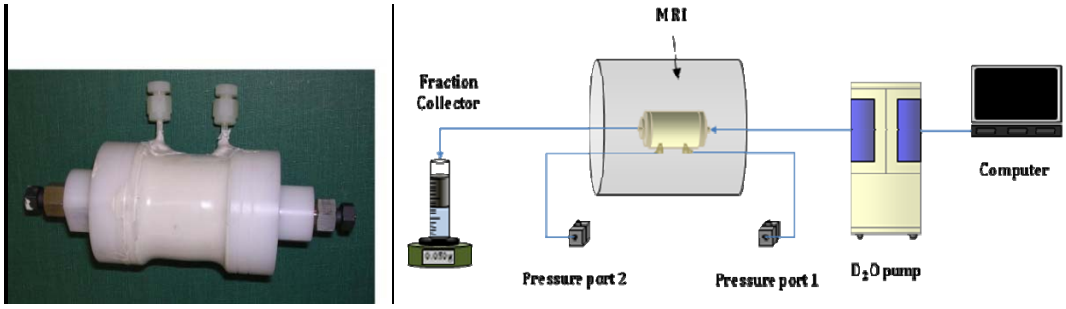

Figure 1. Core with pressure ports (left) and schematics of the experimental setup.

RESULTS AND DISCUSSION

Local pressures and *in situ* fluid saturation distributions from four Portland Chalk core samples were obtained using embedded pressure taps and spin echo MRI during constant pressure waterfloods at different wettabilities. The data were used to identify recovery contributions on the positive and negative sides of the dynamic capillary pressure curve, allowing *in situ* Amott Indices to water to be obtained. The core data from the MRI waterfloods, including injection methods, conventional Amott Indices, end-point saturations and recovery factors, are summarized in Table 3.

Table 3. Core data from MRI waterfloods.

Core	Conventional Amott Index	Injection Method		S_{wi}	Injection Time	Produced Oil	$S_{w,\,or}$	R_f
		Constant Pressure	psi	%PV	h	cm^3	%PV	%OIP
M3	0.39	Water Column	1.2	31.3	43.6	11.0	45.3	20.3
M8	0.45	Pump	5	20.3	42.8	38.0	69.7	62.0
E4	0.17	Pump	5	31.4	88.0	13.2	49.7	26.6
T3	1.00	Water Column	1.2	19.8	41.7	21.0	46.4	33.1

Core Sample M3

Figure 2 shows the oil saturations (black and red) and local pressures (blue and green) in Port 1 and Port 2 for core sample M3 as functions of time. From the figure, the pressure decreases from 0.95 psi to 0.25 psi in Port 1 and from 0.60 psi to 0.20 psi in Port 2 due to spontaneous imbibition of water, as the oil pressure is reduced with increased wetting phase saturation. The pressure is measured in the phase that has higher pressure. The distinct pressure increase at t = 10 hours in Port 1 and at approximately t = 18 hours in Port 2 is believed to represent where the viscous component from the injection pressure in the water phase is recorded, that is, where the water pressure becomes higher than the oil pressure (Pc=0). The Amott Indices to water are calculated by identifying the saturation drop before and after this point:

$$I_{w1} = \frac{10.7}{10.7+13.0} = 0.45 \qquad I_{w2} = \frac{12.7}{12.7+9.5} = 0.57 \qquad (1)$$

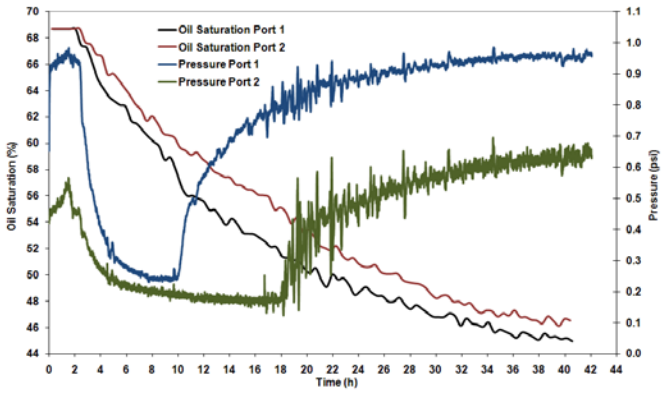

Figure 2. Oil saturations and pressure response in Port 1 and 2 for Core M3.

Core Sample M8

Figure 3 shows the oil saturations and local pressures in Port 1 and Port 2 for core M8 as functions of time. The distinct pressure increase at t = 4 hours in Port 1 and at t = 8.5 hours in Port 2 indicates the point in saturation where Pc=0. Saturations at this point and Amott Indices to water in Port 1 and Port 2 are found from MRI:

$$I_{w1} = \frac{21.8}{21.8+27.0} = 0.45 \qquad I_{w2} = \frac{25.0}{25.0+25.0} = 0.50 \qquad (2)$$

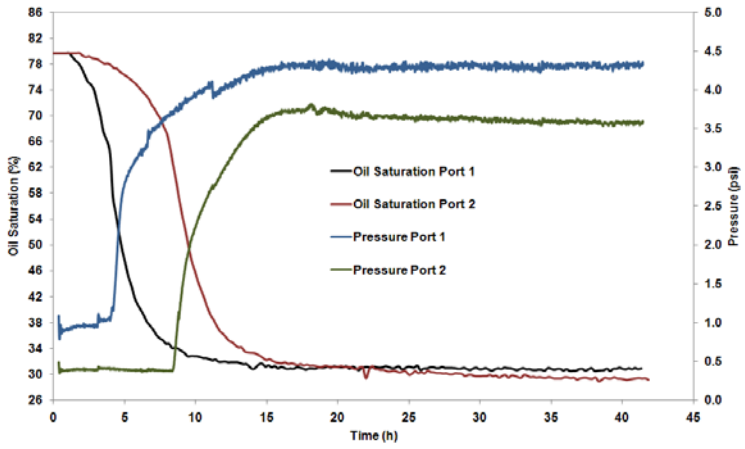

Figure 3. Oil saturations (black and red) and local pressures (blue and green) in Port 1 and Port 2 for Core Plug M8.

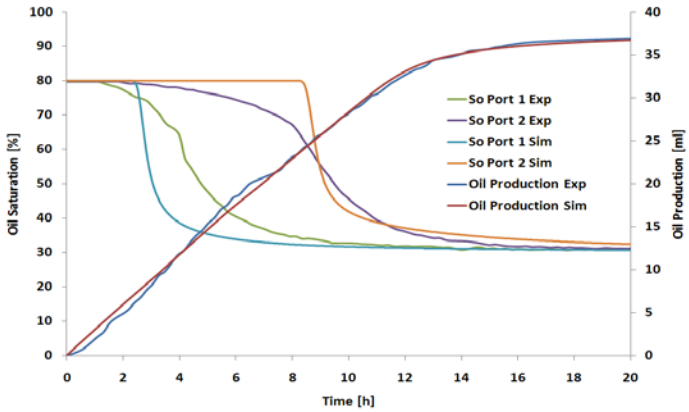

Figure 4. Experimental and simulated oil saturations in Port 1 and 2 and oil production for core sample M8.

The waterflood of core sample M8 was simulated using the core flood simulator *SENDRA* (http://www.ri.reslab.no/sendra.aspx). Experimental and simulated oil production from the core as well as oil saturation is compared in Figure 4. A perfect match was not obtained for the local pressure in the ports; however the simulation captured the key features of the experiments.

Core Sample T3

Figure 7 shows the oil saturations (black and red) and local pressures (blue and green) in Port 1 and Port 2 for core sample T3 as functions of time. From the figure, the pressure drops from 0.9 psi to 0.3 psi in Port 1 and from 0.5 psi to 0.2 psi in Port 2 during imbibition of water. The onset of negative capillary pressure is indicated by the pressure increase at t = 12.5 hours in Port 1 and at t = 14.5 hours in Port 2. The *in situ* Amott Indices to water are calculated for Port 1 and Port 2:

$$I_{w1} = \frac{26.3}{26.3+0.8} = 0.97 \qquad I_{w2} = \frac{26.0}{26.0+0.5} = 0.98 \qquad (3)$$

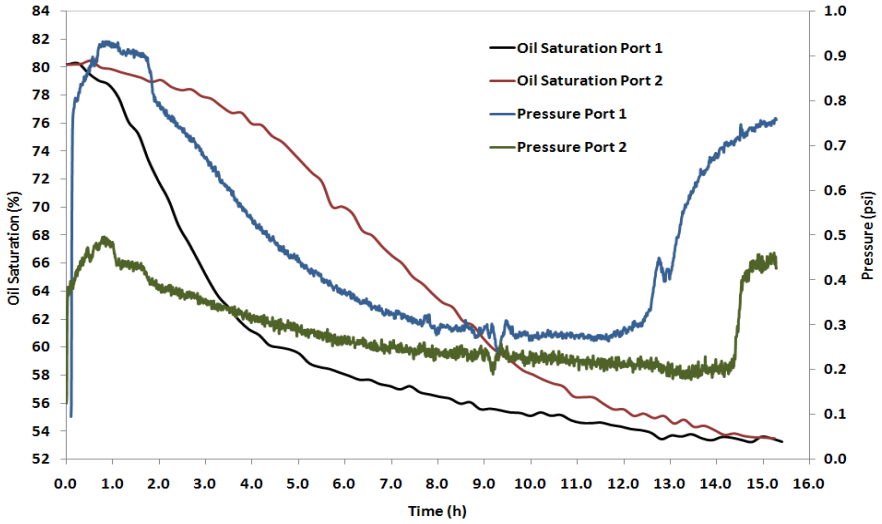

Figure 5. Oil saturations (black and red) and local pressures (blue and green) in Port 1 and Port 2 for Core Plug T3, respectively.

The conventional Amott Indices and the average *in situ* Amott Indices to water for all four core samples are summarized in Table 4.

Table 4. Conventional Amott Indices compared to in situ Amott Indices.

Core Name	Conventional Amott Index [frac.]	*In situ* Amott Index [frac.]	Difference [frac.]
M3	0.39	0.51	0.12
M8	0.45	0.48	0.03
E4	0.17	0.21	0.04
T3	1.00	0.98	- 0.02

Note that the pressure data presented in Figure 2 for core sample M3 are much noisier than the data for core sample M8, E4 and T3. Few saturation data points near the end-point for spontaneous imbibition in Port 1 also create a source of error. The average *in situ* Amott water index for core sample M3 is an estimate based on the best fit in Port 1 and Port 2, but these are less accurate than the other core samples due to the noise.

CONCLUSIONS

Four Portland Chalk core samples at different wettabilities have been waterflooded while measuring local pressures and *in situ* fluid saturations by using high spatial resolution Magnetic Resonance Imaging. The experimental results were used to:

- Identify the separate recovery contributions from spontaneous and viscous displacement
- Calculate *in situ* Amott Indices to water
- Corroborate the conventional Amott Indices well within the margin of error.

ACKNOWLEDGEMENTS

The authors wish to acknowledge the use of the MRI facilities at the ConocoPhillips Technology Center in Bartlesville, OK, USA. Two of the authors are indebted to the Norwegian Research Council.

REFERENCES

Amott, E.: "Observations Relating to the Wettability of Porous Rock." *Petroleum Transactions*, **216**: p. 156-162, 1959.

Aspenes, E., Graue, A. and Ramsdal, J.: "In situ wettability distribution and wetting stability in outcrop chalk aged in crude oil." *Journal of Petroleum Science and Engineering*, **39**: p. 337-350, 2003.

Brautaset, A., Ersland, G., Graue, A.: "In Situ Phase Pressures and Fluid Saturation Dynamics Measured in Waterfloods at Various Wettability Conditions", SPE113510, presented at 2008 SPE/DOE Improved Oil Recovery Symposium, Tulsa, OK, USA, April 20-23, 2008. Accepted for publication in SPEREE.

Donaldson, E. C. and Thomas, R. D.: "Wettability Determination and Its Effect on Recovery Efficiency." *SPE Journal of Petroleum Technology*, **March**: p. 13-20, 1969.

Ekdale, A. A. and Bromley, R. G.: "Trace Fossils and Ichnofabric in the Kjølby Gaard Marl, Uppermost Cretaceous, Denmark." *Bulletin of the Geological Society of Denmark*, **31**: p. 107-119, 1993.

Graue, A.: "Imaging the Effects of Capillary Heterogeneities on Local Saturation Development in Long Corefloods." *SPE Drilling and Completion*, **March**: p. 57-64, 1994.

Graue, A., Aspenes, E., Bognø, T., Moe, R. W. and Ramsdal, J.: "Alteration Of Wettability And Wettability Heterogeneity." *Journal of Petroleum Science and Engineering*, **33**: p. 3-17, 2002.

Graue, A., Viksund, B. G. and Baldwin, B. A.: "Reproducible Alteration Of Wettability Of Low-Permeable Outcrop Chalk", *SPE/DOE Improved Oil Recovery Symposium*, Tulsa, Oklahoma, USA, 1998.

Graue, A., Viksund, B. G., Eilertsen, T. and Moe, R. W.: "Systematic wettability alteration by aging sandstone and carbonate rock in crude oil." *Journal of Petroleum Science and Engineering*, **24**: p. 85-97, 1999.

Morrow, N. R.: "Wettability and Its Effect on Oil Recovery." *SPE Journal of Petroleum Technology*, **December**: p. 1476-1484, 1990.